Environmental Research Letters

OPEN ACCESS

RECEIVED
18 January 2016

REVISED
23 March 2016

ACCEPTED FOR PUBLICATION
29 March 2016

PUBLISHED
19 April 2016

LETTER

Negative elevation-dependent warming trend in the Eastern Alps

M Tudoroiu[1,3], E Eccel[2], B Gioli[4], D Gianelle[1,2,6], H Schume[3], L Genesio[1,4] and F Miglietta[4,5,6]

[1] FOXLAB Joint CNR-FEM Initiative, Via E. Mach, 1 38010 San Michele all'Adige (TN)—Italy
[2] Sustainable Agro-Ecosystems and Bioresources Department, Research and Innovation Centre—Fondazione Edmund Mach, Via E. Mach 1, 38010—San Michele all'Adige (TN), Italy
[3] University of Natural Resources and Life Sciences, Gregor Mendel Strasse 33, A-1180 Vienna, Austria
[4] Consiglio Nazionale delle Ricerche—Instituto di Biometeorologia, via Giovanni Caproni 8—I-50145 Firenze, Italy
[5] Laboratory of Ecohydrology, École Polytechnique Fédérale de Lausanne, CE 3 316 (Centre Est), Station 1, CH-1015 Lausanne, Switzerland
[6] MountFor Project Center, European Forest Institute, c/o Fondazione Edmund Mach, Via E. Mach 1, 38010—San Michele all'Adige (TN), Italy

E-mail: marin.tudoroiu@fmach.it

Keywords: elevation–dependent warming, land use change, solar brightening and dimming

Supplementary material for this article is available online

Abstract

Mountain regions and the important ecosystem services they provide are considered to be very vulnerable to the current warming, and recent studies suggest that high-mountain environments experience more rapid changes in temperature than environments at lower elevations. Here we analysed weather records for the period 1975–2010 from the Eastern Italian Alps that show that warming occurred both at high and low elevations, but it was less pronounced at high elevations. This negative elevation–dependent trend was consistent for mean, maximum and minimum air temperature. Global radiation data measured at different elevations, surface energy fluxes measured above an alpine grassland and above a coniferous forest located at comparable elevations for nine consecutive years as well as remote sensing data (MODIS) for cloud cover and aerosol optical depth were analysed to interpret this observation. Increasing global radiation at low elevations turned out to be a potential driver of this negative elevation–dependent warming, but also contributions from land use and land cover changes at high elevations (abandonment of alpine pastures, expansion of secondary forest succession) were taken into account. We emphasise though, that a negative elevation–dependent warming is not universal and that future research and in particular models should not neglect the role of land use changes when determining warming rates over elevation.

1. Introduction

Mountain regions provide several important ecosystem services, like the protection of human infrastructure or constant supply with high quality drinking water. 40% of Europe's fresh water originates in the Alps supplying tens of millions of Europeans in lowland areas (www.eea.europa.eu). They are important centres of biodiversity and also key targets for tourism and recreation. But the provision of these key services is threatened by climatic changes (Beniston *et al* 1997, Rangwala *et al* 2013).

The term 'elevation–dependent warming' (EDW) typically refers to different warming rates over an altitudinal gradient that might also deviate from the overall global warming rate. This aspect becomes particularly important in the light of the accelerating global warming recorded during the last decades (Hartmann *et al* 2013). Mountain regions which are considered as vulnerable ecosystems (Beniston *et al* 1997) could experience graver changes earlier than the nearby lowlands, if the warming rate is higher in the mountains. For this reason several mountain areas of the world were studied using both, weather station data and modelling approaches, sometimes with contrasting results. Snow/ice cover, clouds, water vapour, aerosols, and soil moisture have been considered as drivers of elevation-dependent warming

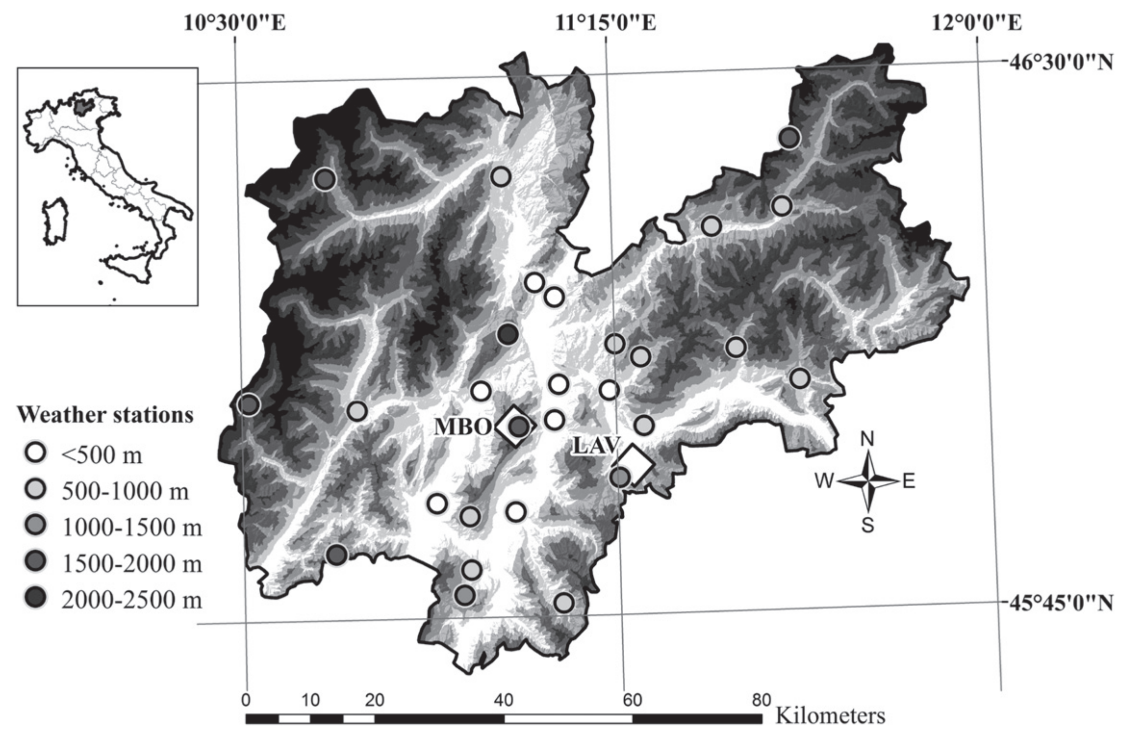

Figure 1. The map of Trentino with 28 weather stations and Eddy covariance (EC) stations at Monte Bondone (MBO) and Lavarone (LAV). The grey scale of the weather stations corresponds to the elevation classes of the digital elevation model (DEM). The altitudes above 2500 m from the DEM are coloured in black.

(Rangwala and Miller 2012). A recent study and meta-analysis by Pepin *et al* (2015) highlighted a trend towards accelerated warming in high elevations, but the authors also admit that this faster warming cannot be considered as universal. Zeng *et al* (2015), in a global perspective, reached an opposite conclusion for some particular mountain regions of the world. More detailed and local analyses using observational data also led to contradictory findings. In some cases a positive elevation dependency of warming was found (Diaz and Eischeid 2007, Liu *et al* 2009, Wang *et al* 2013, Acquaotta *et al* 2015, Wang *et al* 2016) while in other cases opposite results were reported (Pepin & Losleben 2002, Ceppi *et al* 2012, Kirchner *et al* 2013, Philipona 2013). Other studies did not find a clear dependency of the warming rate on elevation (You *et al* 2010, Marty and Meister 2012, Gilbert and Vincent 2013, Gevorgyan 2014, Oyler *et al* 2015). When regional and global climate models were applied the results seemed to converge towards a positive correlation between elevation and warming rate (Qin *et al* 2009, Gobiet *et al* 2014, Rangwala *et al* 2013, Kotlarski 2015, Rangwala *et al* 2015).

This paper reports a series of observations made in the southern part of the Eastern Alps (Province of Trento, Italy) over the last three decades. More specifically it examines how air temperature varied with the altitude and tries to identify possible drivers which lead to the occurrence of the significant negative elevation–dependent warming. This is achieved by bringing together weather records, energy flux measurements, satellite MODIS-data for cloud cover, atmospheric optical depth and inventorial data concerning recent land cover changes in the region.

2. Materials and methods

2.1. Study area and land use

This study was realized in Trentino, a region located in the Central-Eastern Italian Alps, which covers an area of 6212 km^2 comprised between 45°45′–46°30′N and 10°30′–12°00′E (figure 1). This region is characterized by a valley system, the most prominent being the Valley of the river Adige, with a typical elevation range, from bottom to peaks, of about 2000 m. Overall elevation ranges from 70 m to 3769 m. Annual forest inventory data of the last three decades were provided by the 'Servizio Foreste e Fauna' del 'Dipartimento Territorio, Ambiente e Foreste' della Provincia Autonoma di Trento. These data reported the total surface occupied by forests as well as the stocking timber volume.

2.2. Weather data

Homogenised weather data series (Eccel *et al* 2012) for mean (T_{mean}), maximum (T_{max}) and minimum (T_{min}) daily air temperatures, and incoming radiation were obtained from the Meteorological service of the Autonomous Province of Trento-PAT and from Fondazione Edmund Mach. In total a number of 28 weather stations between 84 and 2125 m a.s.l. were considered (supplementary table S1) for the period January 1975 until December 2010. The data for incoming radiation were available for a lower number of stations and years (some low elevation stations have data starting in 1983 while the records for high elevation stations only start after 1999) (supplementary table 1, supplementary figure 3). The weather stations were first divided into low and high elevation using the median of the elevations as separation threshold. Changes in mean air temperature for the considered time interval were studied for the two groups. Furthermore altitudinal gradients of temporal trends were estimated for T_{mean}, T_{min} and T_{max} by linear regression. Two seasonal sub-periods were also considered: from November to April (A) and from May to October (B). November till April (period A), is the period when snow cover prevails at altitudes above the median elevation of the two groups with some obvious variability among different years. Changes in global solar radiation were examined for 3 stations located at low elevation (supplementary table 1, supplementary figure 3) (San Michele—205 m, Arco —84 m a.s.l., Trento Sud—185 m a.s.l) and 3 located at high elevation (Monte Bondone—1552 m a.s.l., Baselga di Pinè—983 m a.s.l., Tremalzo—1560 m a.s.l.). A data-driven procedure was used to calculate changes in the transmissivity of the atmosphere at each station. The values of the first year in each series (1983 for low elevation and 2000 for high elevation) were used to construct the daily courses of theoretical clear sky days month by month. For that purpose we assembled the highest radiation values measured for each hour of the day within a month (excluding the twilight hours) to a daily course and corrected the values according to the Sun declination for each day. Finally, the monthly and then yearly courses of hourly radiation under clear sky conditions were reconstructed for each individual station. The difference (ΔRad) and the ratio (Rrad) between each daily mean of incoming radiation and the corresponding maximum radiation under clear sky conditions in the first year of the series were calculated for the whole dataset (1983–2010 for the low elevation stations and 2000–2010 for the high elevation stations). This procedure yielded robust data to assess changes in radiative input over the years for different elevations, minimising the effect of different aspects, local topography and possible errors due to imperfect cross-calibration of the solar sensors.

2.3. Flux data

Surface energy flux data for different land cover types at high elevation were obtained from two Eddy Covariance stations (figure 1): Monte Bondone (MBO) and Lavarone (LAV). MBO (46°00°53″ N, 11° 02′45″ E) is installed above an alpine pasture where the main species is *Nardum stricta* with a mean canopy height of 0.3 m, located at 1553 m a.s.l while LAV (45° 57′ 23″ N, 11° 16′ 52″ E) is installed above an evergreen forest of Silver fir (*Abies alba Mill.*) and Norway spruce (*Picea abies L.*) -with an average height of 28 m, located at 1349 m a.s.l. Both stations are part of the Fluxnet Network and are equipped for measuring CO_2 fluxes, water vapour and ancillary meteorological parameters (Marcolla *et al* 2011, Sakowska *et al* 2014). Measurements started in 2002 in LAV and in 2003 in MBO. Fluxes were computed according to the Fluxnet Methodology (Baldocchi *et al* 2001) in order to obtain half-hourly data. Daily averages of latent and sensible heat flux (LE and H), net radiation (Rn) and albedo were calculated for both ecosystems over a 9 year period. In order to compare the air temperature and their changes at different heights, daily potential air temperatures (T_{Pot}) were calculated according to equation (1).

$$\frac{T_0}{T} = \left(\frac{p_0}{p}\right)^{0.286} \tag{1}$$

where T_0 is the absolute temperature at the higher pressure in K, T is the absolute temperature at the lower pressure in K, p_0 is the higher pressure, and p is the lower pressure.

Aerodynamic resistance to water vapour transfer Ra,v was computed using the equation:

$$R_{a,v} = R_{a,m} + R_b = \frac{u}{u_*^2} + \frac{2}{ku_*}\left(\frac{Sc}{Pr}\right)^{\frac{2}{3}} \tag{2}$$

Where $R_{a,m}$ is the resistance to momentum transfer (s m^{-1}), R_b the resistance of the quasi-laminar boundary layer resistance (s m^{-1}) (Verma 1989, Baldocchi and Ma 2013), u is wind velocity in m s^{-1}, k is von Karman's constant (0.4), u^* is friction velocity in m s^{-1}, Sc is the dimensionless Schmidt number and Pr is the Prandtl number.

2.4. Remote sensing data

Monthly time series of MODIS Terra Level 3 data for cloud fraction (Monthly MOD08_M3.051) (Acker and Leptoukh 2007) were obtained from NASA GES DISC (http://disc.sci.gsfc.nasa.gov/giovanni). Day and night time cloud cover was analysed in comparison for different paired valley and mountain areas (see supplementary table S2, supplementary figure 2) for the whole period since MODIS was operational (March 2000–December 2014). Averages were calculated for the mountain and valley areas and the differences between the two categories (mountain—valley) were analysed over time (figure 6). Monthly means for aerosol optical depth (AOD) were retrieved form neo.sci.gsfc.nasa.gov (Product ID MOD04/MYD04) for the period 2003–2013 and for pixels corresponding to the same location of the weather stations used for irradiance analysis. The AOD trend over time was studied and furthermore correlated with the difference between the measured incoming radiation and the corresponding clear sky radiation in the first year of the series (ΔRad).

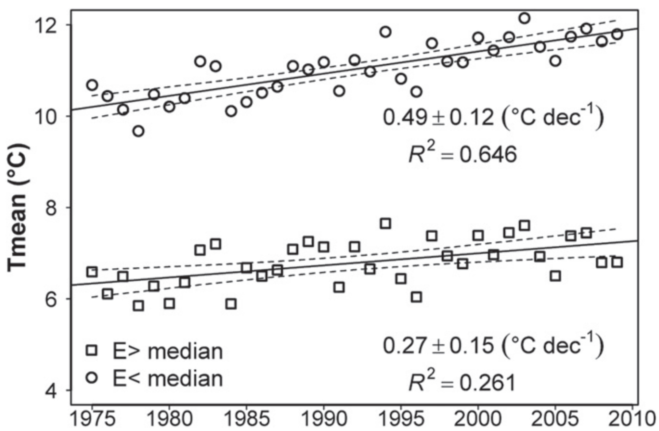

Figure 2. Temperature trends at high versus low elevation (E > median and E < median) within the studied period. The dashed lines indicate the 95% confidence interval. Regressions are significant at $p = 0.001$ and $p = 0.0004 \times 10^{-5}$ for high and low elevation, respectively. The slope of linear regression and coefficients of determination are shown in the figure, where the slope indicates rate of temperature increase in °C decade^{-1}.

3. Results

Weather data for the study region (figure 1) show that over the last 35 years annual mean air temperature increased both at low and high elevation, but the rate of change was not equal (figure 2). On average the rate of temperature increase was significantly higher at low compared to high elevation (0.49 ± 0.12 and 0.27 ± 0.15 °C decade^{-1}, respectively). A significant negative correlation was found between the elevation and the observed rate of change in air temperature over the last 35 years (figure 3). This trend is consistent for the different seasons and for the maximum, minimum and mean daily temperature values (T_{max}, T_{min}, T_{mean}). For the two periods considered (A: November–April, and B: May–October 1975 to 2010) the warming rate of the mean temperatures (ω, T_{mean}) decreased with height by 0.26 ± 0.11 °C decade^{-1}km^{-1} and 0.22 ± 0.08 °C decade^{-1}km^{-1}, respectively. The decrease in warming rate with height for minimum temperatures (ω T_{min}) was 0.20 ± 0.11 decade^{-1}km^{-1} for the snow covered period (A) and 0.15 ± 0.09 °C decade^{-1}km^{-1} for the snow-free period (B). The corresponding values for maximum temperature (ω T_{max}) were 0.33 ± 0.17 °C decade^{-1}km^{-1} and 0.28 ± 0.16 °C decade^{-1}km^{-1} for the snow covered period (A) and for the snow free period (B), respectively. It is worth noting that in all cases the decrease in warming rate with height was more pronounced in the snow covered period (A). The daily deviations of radiative input from the potential input under clear sky conditions at the beginning of data recording (ΔRad) decreased for the low elevation stations on average by 1.68 ± 0.25 Wm^{-2} year^{-1} for the period 1983–2010 (figure 4). Instead, an increase of 2.7 ± 1.3 W m^{-2} year^{-1} (figure 4) was observed at high-elevation stations, even though for a shorter period (2000–2010).The changes in ΔRad were more pronounced for clear sky days in all elevations (table 1).

Significant differences were also observed regarding the turbulent fluxes above two representative high elevation land use types from Trentino: 'coniferous forest' (covering 50% of the total area of the province) and 'alpine grassland' (17% of the total area of the province) (Servizio Foreste e Fauna PAT) located at comparable elevations (1349 and 1553 m a.s.l, respectively). When averaged over the whole measurement period of 9 years, the latent heat flux was higher in the evergreen forest by 10.8 ± 1.7 W m^{-2} (figure 5(a)), with the largest positive mean difference in March (56.4 W m^{-2}) and the most negative in late May (−33.2 W m^{-2}). The sensible heat flux over the forest was higher than over the grassland for the entire measurement period (38.2 ± 2.6 W m^{-2}) except for late autumn and winter, when the differences were negligible (figure 5(b)). Overall the total turbulent energy exchange (H + LE) was higher over forest, which clearly represents the rougher vegetation form with the lower resistance to turbulent transfer (figure 5(d)).

The difference in potential air temperature between the forest and the grassland (calculated as forest minus grassland), averaged for the 9 year period on a daily basis, was 0.13 ± 0.04 °C (figure 5(e)). T_{Pot} was higher over the forest during late autumn and winter with the highest value in January (+1.60 °C) but lower from early spring to mid-November. The highest negative difference was recorded in October (−0.63 °C). For the snow free period (B) the difference was negligible (−0.009 °C ± 0.1) while for the snow covered period (A) it equalled 0.25 ± 0.16 °C. When averaged on a half-hourly basis, the air above the forest stand turned out to be cooler around noon and in the afternoon hours during the snow free period (period B), but clearly warmer at night time all year long. The temperature amplitude was always smaller in case of

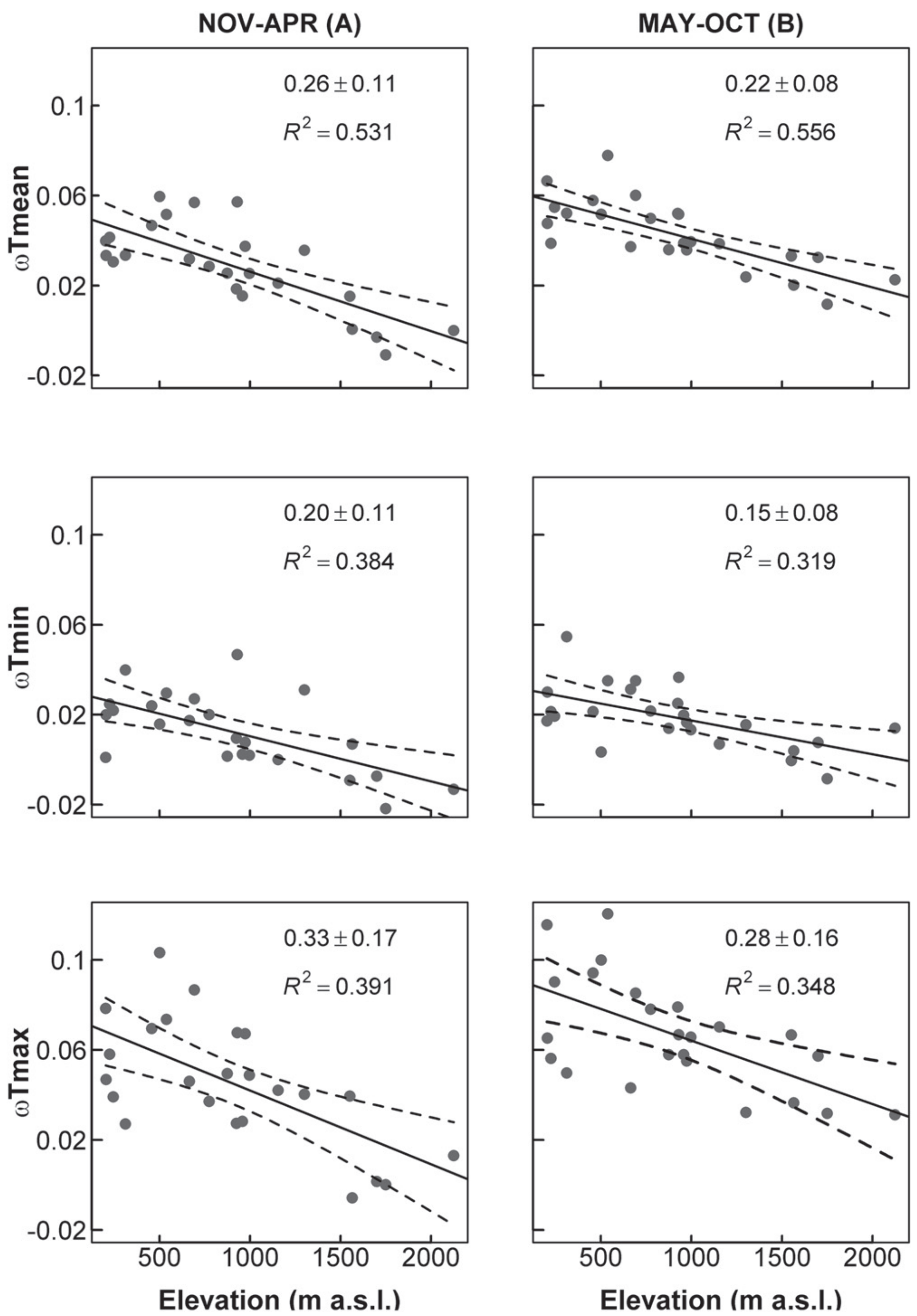

Figure 3. Air temperature changes over elevation, for mean, minimum and maximum temperatures (ωT_{mean}, ωT_{min}, ωT_{max}), separately for the period November to April (A), and the period May to October (B). The dashed lines indicate the 95% confidence interval. Slopes of linear regressions and the coefficients of determination are shown in the figure, while the slope of linear regression indicates the rate of air temperature change in °C decade-^{1}km^{-1}. Regressions are significant at $p < 0.05$.

the forest (supplementary figure 1). The albedo values were consistently lower for the forest, resulting in an overall 37.26 ± 2.03 W m^{-2} higher net energy gain (figure 5(c)). During the snow free period mean albedo values of 0.10 ± 0.00 and 0.24 ± 0.01 were obtained for the forest and the grassland, respectively. The biggest difference of 0.72 between the two ecosystems was recorded in the snow covered period (A) (figure 5(f)).

The analysis of MODIS-satellite data revealed that monthly means of cloud cover hardly varied over the period 2000 to 2014 both for night and day time (figure 6). The difference in cloud cover fraction (high minus low elevation) over time was always positive during day time. The dimensionless Aerosol Optical Depth (AOD) at low elevation constantly decreased for the period 2003–2013 by 0.005 ± 0.002 year^{-1} (figure 7) and by 0.008 ± 0.004 for the period

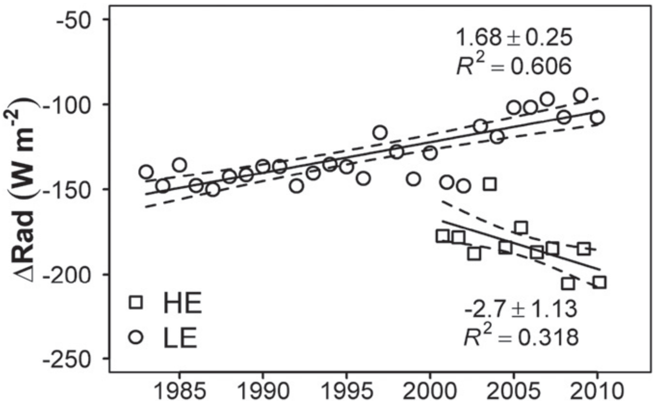

Figure 4. Changes in mean annual difference between the measured incoming radiation and the corresponding 'clear sky' radiation in the first year of the series (ΔRad) for low elevation (LE—empty circles) and high elevation (HE—empty squares). The dashed lines show the 95% confidence intervals. Slopes of linear regressions and the coefficients of determination are shown in the figure, the slope of linear regression indicating the rate of change in ΔRad in W m^{-2} year^{-1}. The low elevation values were obtained by averaging the records from Arco, Trento and San Michele (for the period 1983–2010), while the high elevation values by averaging the records from Monte Bondone, Baselga di Piné and Tremalzo (for the period 2000–2010).

Table 1. Rate of change in mean annual difference between the measured incoming radiation and the corresponding clear sky radiation in the first year of the series (ΔRad, W m^{-2}) for low and high elevation. *s* is the slope of linear regression for ΔRad over the studied period. Statistics are computed for three categories. All days (includes all the days of all the years), partially cloudy days (the ratio between the measured incoming radiation and the corresponding clear sky radiation in the first year of the series—Rrad—was >40% of the maximum Rrad), clear sky days (Rrad > 60% of the maximum Rrad). Low elevation: averages of Arco, Trento and San Michele, High elevation averages for Monte Bondone, Baselga di Piné and Tremalzo.

	Low elevation		High elevation	
	s (W m^{-2} year^{-1})	R^2	s (W m^{-2} year^{-1})	R^2
All days	1.68 ± 0.54	0.61	−2.68 ± 2.97	0.32
Partially cloudy days	1.64 ± 0.44	0.69	−2.75 ± 1.70	0.60
Clear sky days	1.75 ± 0.44	0.76	−2.99 ± 2.14	0.53

2003–2010. AOD and ΔRad for clear sky days are well correlated ($R^2 = 0.72$, figure 8).

4. Discussion

In the period 1975–2010 the air temperature over land increased at a rate of 0.30 °C decade^{-1} (Rangwala *et al* 2013). Our analysis of air temperature data from 24 meteorological stations along an elevation gradient revealed a significant negative correlation between the warming rate and the elevation for the same temporal span. This finding confirms previous results reported by Philipona (2013) for the Swiss Alpine region. The two studies are similar with respect to the large number of stations located at different altitudes, the elevation range and the time span covered. The decreasing warming rates (ω) over elevation were slightly more pronounced in the Swiss study with 0.52 and 0.35 °C decade^{-1} for low and high elevations, respectively, which is 0.03 and 0.08 °C decade^{-1} higher than in Trentino (table 2). These small differences, which fall into the confidence limits of the regressions, can be a result of the different time intervals considered and/or of the higher mean elevation of the Swiss weather stations for low and high elevation. Despite the robustness of both data sets, however, the concept of a negative elevation-dependent warming cannot be simply generalised to other mountain ranges of Europe and the world. Major inconsistencies remain with other studies as well as with a series of selected modelling approaches (Gobiet *et al* 2014, Rangwala *et al* 2013, Kotlarski 2015).

The lack of an unequivocal positive or negative sign in ω definitely requires additional efforts to interpret the apparent contradiction in our results and to understand the causes of the observed negative trends. Both Philipona (2013) and Zeng *et al* (2015) attributed the occurrence of a negative ω to the increase in solar brightening at low elevations, a phenomenon which is generally attributed to an overall reduction in atmospheric pollution sources. In mountainous areas this reduction took place exclusively in the denser populated valleys. A substantial reduction of anthropogenic secondary aerosols and particulate matter in the atmosphere can actually lead to an increase in atmospheric transmissivity and thus to enhanced radiative forcing at the surface leading to warming (Arneth *et al* 2009, Philipona *et al* 2009). Such a 'solar brightening effect' has been described also for the Greater Alpine Region by Auer *et al* (2007) and for the north of Italy by Manara *et al* (2015). Our analysis of radiation

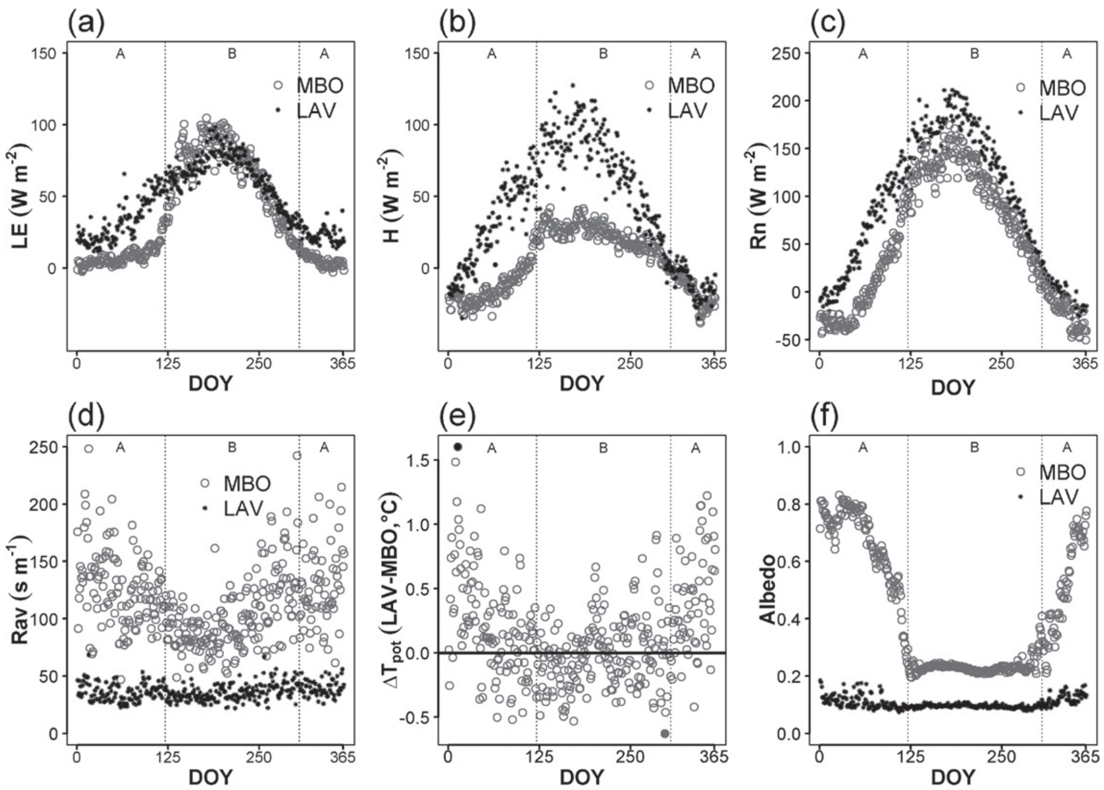

Figure 5. Daily means for 9 years from eddy covariance measurements over a coniferous forest (Lavarone—LAV) and an alpine grassland (Monte Bondone—MBO) (a) Annual courses of latent heat flux (LE), (b) annual courses of sensible heat flux (H), (c) annual courses of net radiation (Rn), (d) annual courses of aerodynamic resistance to water vapour transfer (Rav), (e) the difference in potential air temperature (ΔT_{pot}) calculated as forest (LAV) minus grassland (MBO); the most negative difference (−0.63 °C, October) and the most positive difference (+1.6 °C) are highlighted by full grey and full black dots, respectively; (f) annual courses of albedo. The vertical dashed lines show the separation into snow covered (A) and snow free (B) periods.

data from three low-altitude weather stations of Trentino, which continuously measure solar irradiance since 1983 (Arco, San Michele and Trento), strongly support this explanation. The mean annual difference between hourly incoming radiation and the maximum hourly radiation under potential clear sky conditions in the first year of the Trentino's series (ΔRad) decreased over time (figure 4) at a rate of $1.69 \pm 0.25\ \mathrm{W\ m^{-2}\ year^{-1}}$. This decrease in ΔRad shows in fact an increase in 'solar brightening' (the atmosphere getting closer to the clear sky conditions) and is in the same order of magnitude with the values reported by Manara *et al* (2015) for the North of Italy. Most of the effect is attributable to increased atmospheric transmissivity on clear sky days (table 1). Brightening under clear sky conditions is further confirmed for the period 2003 till 2010 by MODIS-AOD data, which indicate a concomitant decline in satellite-measured aerosol optical depth (AOD) for the locations of the three weather stations (figure 7). Consequently, ΔRad for clear sky days and MODIS-AOD values are very well correlated (figure 8), allowing a quantitative estimate of the relation between atmospheric optical depth and incoming shortwave radiation for the latitude of the study area and for the specific wavelength used by MODIS for AOD estimation.

Solar brightening at low elevation is *per se* sufficient to explain the observed negative sign of ω, but only under the assumption that no warming compensatory effects occurred at high elevations. In this context special attention has to be granted to implications associated with the observed land use change at high elevations in the Alps. The extensive reforestation programme after the end of the Second World War (Fuchs *et al* 2013) and more recently the wide-spread abandonment of alpine pastures led to a significant expansion and regrowth of forests (Guidi *et al* 2014, Tasser *et al* 2007). Baur (2013) reports that the forest area increased by 8% in Switzerland between 1985 and 2005. In Trentino the forest area increased by 13.7% over the period 1976–2010, while the stocking forest biomass nearly doubled (+41.5%). 75% of the increase in forest area occurred at elevations above 800 m (Sitzia 2009).

It is well known that forests have a lower albedo than grasslands and meadows and this unavoidably leads to a higher absorption of shortwave solar radiation (de Wit *et al* 2014). For instance, the albedo of an alpine grassland in Tyrol ranged between 0.20 and 0.25 during the growing season (Hammerle *et al* 2008). Betts and Ball (1997) report a mean summertime value of 0.20 for grasslands. On the other hand, literature values for spruce forests, vary between 0.08 and 0.12

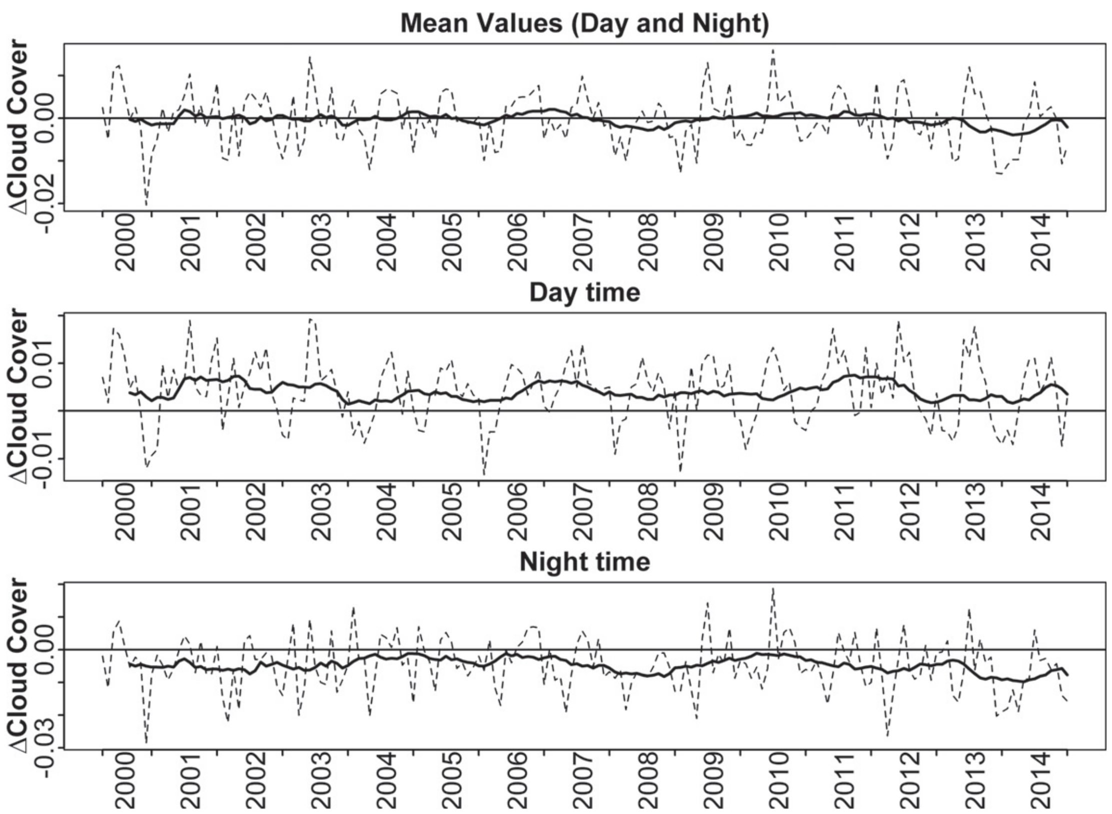

Figure 6. MODIS monthly differences of cloud fraction between upland and lowland for mean values (A) day time (B) and night time (C). Mean differences were calculated for three paired lowland and upland sites. Dashed line: indicates the monthly means while the solid line shows twelve-months moving average.

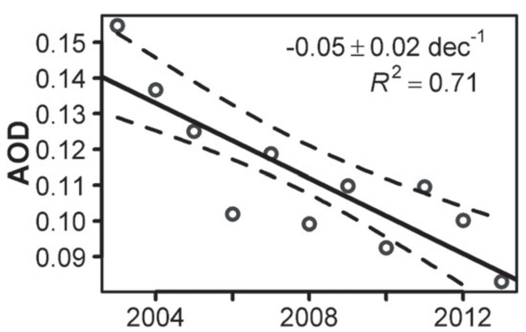

Figure 7. Annual means of MODIS aerosol optical depth for low elevation sites. The dashed lines indicate the 95% confidence intervals. Slopes of linear regressions and the coefficients of determination are shown in the figure, the slope of linear regression indicating the mean rate of change in AOD for the period 2003–2013.

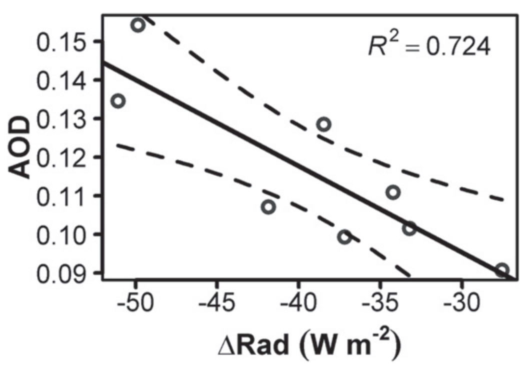

Figure 8. Correlation between the annual mean MODIS aerosol optical depth (AOD) and mean annual difference between the measured incoming radiation and the corresponding clear sky radiation in the first year of the series (ΔRad, W m^{-2}) for low elevation in clear sky conditions. The clear sky days are considered days when the ratio between the measured incoming radiation and the corresponding clear sky radiation in the first year of the series (Rrad) was at least 60% of the maximum value of Rrad. Coefficient of determination is shown in the figure.

(e.g. Eck and Deering 1992, Betts and Ball 1997, Lukeš *et al* 2013). All the quoted albedo values are in good accordance with our findings (snow free period values of 0.10 ± 0.00 for the mixed Silver fir and Norway spruce forest and 0.24 ± 0.01 for the grassland). This difference could explain the large net radiation difference between an alpine grassland and a subalpine spruce forest in the Bernese Oberland (Switzerland) measured by Eugster and Cattin (2007). In comparison to the grassland the net gain of the darker forest canopy was a 110 W m^{-2} for the three summer months. So accordingly, a land use shift from pasture to forestry results in a higher net radiation and higher heat flux rates to the atmosphere, which becomes clearly evident from our results.

Compared to other land use types, the exchange of sensible and latent heat between forests and the

Table 2. Comparison between the weather data of Trentino and data reported by Philipona (2013) for Switzerland. For both regions, information concerning altitudinal range, number of stations, mean air temperature (T_{mean}) and rate of change in air temperature are presented separately for high and low elevation.

Region	Period	Altitudinal range (m asl)		Number of stations		T_{mean} (°C)		Rate of change (ωT_{mean}, °C decade^{-1})	
		low	high	low	high	low	high	low	high
Trentino	1976–2010	203–875	925–2125	12	12	11	6.8	0.49	0.27
Switzerland	1980–2005	203–776	1427–3580	25	10	9.8	0.7	0.52	0.35

atmosphere is indeed much more efficient, as forests have a higher surface roughness leading to an enhanced mechanical turbulence (Baldocchi and Ma 2013). This reduced aerodynamic resistance to heat transfer can be noticed also from the data of the two flux towers used in this study (figure 5(d)). Eugster and Cattin (2007) observed that most of the higher net energy input at the forest site was used for evapotranspiration resulting in cooler day time conditions. But this effect was more than offset by the fact that open areas like grasslands lose more sensible heat to cold-air drainage flows at night. As a consequence, on a seasonal basis, the mean air temperature above the subalpine coniferous forests was 1.1 °C higher than above the grassland.

However, the relations might change with the admixture of deciduous tree species. Results from 27 Fluxnet sites in the temperate zone of Europe and the US show that the mean summertime (June till August) Bowen ratio for deciduous forests (0.43) was clearly lower than that of coniferous forests (1.07) expressing the higher water consumption (i.e. higher latent heat flux) of deciduous trees (Wilson *et al* 2002). Additionally, forests may have higher transpiration rates over a longer time compared to non-forested areas due to deeper rooting of the trees, which grants them access to water resources that are not accessible to grasses (Pielke 2005, Mahmood *et al* 2014). The resulting shift in energy partitioning towards latent heat flux is supposed to cool the air (Ban-Weiss *et al* 2011).

Finally, taking also wintertime into account, the presence of forests drastically reduces the surface albedo (e.g. Betts and Ball 1997) by shortening the overall duration of surface snow cover, while prolonged snow cover occurs at pastures and meadows. In summary the net effect of forest expansion on near-surface air temperature is a balance between three components: albedo, surface roughness (by enhancing turbulent fluxes) and evapotranspiration. Past studies have shown that air warming effects of afforestation are likely to prevail in dry regions (Peng *et al* 2014) or snow rich areas (de Wit *et al* 2014, Schwaab *et al* 2014), while the opposite may occur in the tropics and temperate, non-water limited regions, where enhanced latent heat fluxes may counterbalance albedo which potentially contributes to local warming (Bonan 2008, Anderson *et al* 2011, Gálos *et al* 2013, Yunusa *et al* 2015).

The data from the two Eddy covariance stations in Monte Bondone (MBO, alpine grassland) and in Lavarone (LAV, mature coniferous forest), continuously operated for the period 2004–2012, provide reliable information in this respect. Daily means calculated over 9 years indicate that prolonged wintertime snow cover at the grassland site substantially reduced wintertime sensible heat flux (H) compared to the conifer forest in Lavarone (figure 5(b)). The lower albedo of the forest together with its higher net radiation (figures 5(c) and (f)) led to a higher mean sensible heat flux (H, figure 5(b)). Latent heat flux (LE) was instead not very different between the two land cover types (figure 5(a)). As a consequence, near-surface air temperature was observed to be higher over the forest by 1.7 ± 0.3 °C, even after considering the elevation difference between the two stations by calculating the potential air temperatures (0.13 °C ± 0.03). However, it is worth noting that even though the mean air temperature (9 year average) was higher above the forest, the warming rate above the two land use types was similar (data not shown).

Apart from the pronounced carbon sequestration effect of forests that counteracts warming on a larger scale, forests may still affect atmospheric properties and the local climate in other ways. The hypothesis that forests can directly contribute to the formation of clouds (Heiblum *et al* 2014) and haze is stimulating debates and new studies in the scientific community. The 'biotic pump' concept (Makarieva and Gorshkov 2007, Makarieva *et al* 2013) claims that a physical mechanism leading to reduced atmospheric pressure over forests creates advection of moist air over long distances. The 'bioprecipitation' concept (Morris *et al* 2014) assumes instead that ice nucleating airborne microorganisms or bacterial/fungal compounds, which are emitted by forests, might have a detectable cloud or haze formation effect. Moreover forests are net emitters of Biogenic Volatile Organic Compounds (BVOCs) (Unger 2014, Maja 2015), which are precursors of secondary organic aerosol (SOA) formation (Fuzzi *et al* 2015, Jokinen *et al* 2015) affecting light absorbance, transmittance and reflectance of the atmosphere, and thus probably diminishing the radiative forcing (Ruckstuhl *et al* 2008, Spracklen *et al*

2008). BVOC fluxes are proportional to the relative fraction of the land which is covered by forests and to their net emission rates of BVOCs, which have been shown to correlate in turn with forest leaf area (Kulmala *et al* 2004). In this light the increasing deviation of the incoming radiation from radiation under clear sky conditions (ΔRad) at the three weather stations above 950 m (figure 6) could be a hint to enhanced SOA formation in high elevations, where the forest area had increased most. But facing only a short measurement series (2000–2010) and not having direct measurements of BVOC emissions or SOA formation, this interpretation remains speculative.

5. Conclusions

The data presented in this paper reinforce the view already expressed by Pepin *et al* (2015) that a positive elevation-dependent warming is not universal in mountain regions. In addition, our findings confirm the opposite hypothesis of e.g. Zeng *et al* (2015) and Philipona (2013), who attributed a negative elevation-dependent warming to solar brightening and increased radiative forcing at lower elevations. Even though a direct relationship between the observed warming trends and increasing forest cover at high elevation could not be identified, this study illustrates the potential of afforestation to compensate or amplify elevation-dependent warming trends by changing the biophysical surface properties of the landscape (roughness, albedo). Eventually, it would be desirable to develop best management practices for forested mountain regions with respect to climate change mitigation strategies, for instance as concerns the forest management form (e.g. single selection system, clear cutting system), the choice of tree species or the stand density.

Similar to other EDW studies, the absence of very elevated weather stations with long term records restricted our analyses to altitudes below 2125 m. Covering an altitudinal gradient of 2040 m this study provides a good estimate of the trend for the managed range (forest and pasture), but still we missed roughly 1600 m to the maximum peak height of the region. This limitation calls for better future assessments of meteorological parameters at very high elevations despite the harsh environment and associated methodological problems.

Acknowledgments

The study was realized within a PhD project supported by FIRS>T (FEM International Research School) and contributes to the objectives of the FP7 Project AIRFORS (Contract no. 286079). It also contributes to the objectives of MountFor, a Project Centre of the European Forest Institute (EFI). We also thank Meteotrentino (PAT), Barbara Marcolla, Matteo Sottocornola, Roberto Zampedri, 'Servizio Foreste e Fauna' of PAT and Gianantonio Battistel. MODIS mission scientists and associated NASA personnel are acknowledged for the production of the MODIS cloud cover and AOD data used in this paper.

References

Acker J G and Leptoukh G 2007 Online analysis enhances use of NASA Earth science data *EOS Trans. Am. Geophys. Union* **88** 14

Acquaotta F, Fratianni S and Garzena D 2015 Temperature changes in the North-Western Italian Alps from 1961 to 2010 *Theor. Appl. Climatol.* **122** 619–34

Anderson R G *et al* 2011 Biophysical considerations in forestry for climate protection *Front. Ecol. Environ.* **9** 174–82

Arneth A, Unger N, Kulmala M and Andreae M O 2009 Atmospheric science. Clean the air, heat the planet? *Science* **326** 672–3

Auer I *et al* 2007 HISTALP—Historical instrumental climatological surface time series of the Greater Alpine Region *Int. J. Climatol.* **27** 17–46

Baldocchi D *et al* 2001 FLUXNET: a new tool to study the temporal and spatial variability of ecosystem-scale carbon dioxide, water vapor, and energy flux densities *Bull. Am. Meteorol. Soc.* **82** 2415–34

Baldocchi D and Ma S 2013 Use affect air temperature in the surface boundary layer? Lessons learned from a comparative study on the energy balance of an oak savanna and annual grassland *Tellus* B **65** 1–22

Ban-Weiss G A, Bala G, Cao L, Ong, Pongratz J and Caldeira K 2011 Climate forcing and response to idealized changes in surface latent and sensible heat *Environ. Res. Lett.* **6** 034032

Baur P 2013 La superficie forestale in Svizzera aumenta *Montagna* **4** 11–4

Beniston M, Diaz H F and Bradley R S 1997 Climatic change at high elevation sites: an overview *Clim. Change* **36** 233–51

Betts A K and Ball J H 1997 Albedo over the boreal forest *J. Geophys. Res.* **102** 901–9

Bonan G B 2008 Forests and climate change: forcings, feedbacks, and the climate benefits of forests *Science* **320** 1444–9

Ceppi P, Scherrer S C, Fischer A M and Appenzeller C 2012 Revisiting Swiss temperature trends 1959–2008 *Int. J. Climatol.* **32** 203–13

Diaz H F and Eischeid J K 2007 Disappearing 'alpine tundra' Köppen climatic type in the western United States *Geophys. Res. Lett.* **34** L18707

Eccel E, Cau P and Ranzi R 2012 Data reconstruction and homogenization for reducing uncertainties in high-resolution climate analysis in Alpine regions *Theor. Appl. Climatol.* **110** 345–58

Eck T F and Deering D W 1992 Canopy albedo and transmittance in a spruce-hemlock forest in mid-September *Agric. For. Meteorol.* **59** 237–48

Eugster W and Cattin R 2007 Evapotranspiration and energy flux differences between a forest and a grassland site in the subalpine zone in the Bernese Oberland *Erde* **138** 237–56

Fuchs R, Herold M, Verburg P H and Clevers J G P W 2013 A high-resolution and harmonized model approach for reconstructing and analysing historic land changes in Europe *Biogeosciences* **10** 1543–59

Fuzzi S, Baltensperger U, Carslaw K, Decesari S and Gon H D Van Der 2015 Particulate matter, air quality and climate: lessons learned and future needs *Atmos. Chem. Phys.* **15** 8217–99

Gálos B, Hagemann S, Hänsler A, Kindermann G, Rechid D, Sieck K, Teichmann C and Jacob D 2013 Case study for the assessment of the biogeophysical effects of a potential afforestation in Europe *Carbon Balance Manag.* **8** 3

Gevorgyan A 2014 Surface and tropospheric temperature trends in Armenia *Int. J. Climatol.* **34** 3559–73

Gilbert A and Vincent C 2013 Atmospheric temperature changes over the 20 th century at very high elevations in the European Alps from englacial temperatures *Geophys. Res. Lett.* **40** 2102–8
Gobiet A, Kotlarski S, Beniston M, Heinrich G, Rajczak J and Stoffel M 2014 21st century climate change in the European Alps—a review *Sci. Total Environ.* **493** 1138–51
Guidi C, Vesterdal L, Gianelle D and Rodeghiero M 2014 Changes in soil organic carbon and nitrogen following forest expansion on grassland in the Southern Alps *For. Ecol. Manage.* **328** 103–16
Hammerle A, Haslwanter A, Tappeiner U, Cernusca A and Wohlfahrt G 2008 Leaf area controls on energy partitioning of a mountain grassland *Biogeosciences* **5** 421–31
Hartmann D L, Klein Tank A M G, Rusticucci M, Alexander L V, Brönnimann S, Charabi Y, Dentener F J, Dlugokencky E J, Easterling D R, Kaplan A, Soden B J, Thorne P W, Wild M and Zhai P M 2013 Observations: atmosphere and surface *Climate Change 2013: The Physical Science Basis. Contribution of Working Group I to the Fifth Assessment Report of the Intergovernmental Panel on Climate Change* (Cambridge: Cambridge University Press) ch 2 pp 159–254
Heiblum R H, Koren I and Feingold G 2014 On the link between Amazonian forest properties and shallow cumulus cloud fields *Atmos. Chem. Phys.* **14** 6063–74
Jokinen T, Berndt T, Makkonen R, Kerminen V, Junninen H and Paasonen P 2015 Production of extremely low volatile organic compounds from biogenic emissions: measured yields and atmospheric implications *Proc. Natl Acad. Sci. USA* **112** 1–6
Kirchner M, Faus-Kessler T, Jakobi G, Leuchner M, Ries L, Scheel H-E and Suppan P 2013 Altitudinal temperature lapse rates in an Alpine valley: trends and the influence of season and weather patterns *Int. J. Climatol.* **33** 539–55
Kotlarski S 2015 The elevation dependency of 21st century European climate change: an RCM ensemble perspective *Int. J. Climatol.* **35** 3902–20
Kulmala M, Suni T, Lehtinen K E J, Dal Maso M, Boy M, Reissell A, Rannik Ü, Aalto P, Keronen P, Hakola H, Bäck J, Hoffmann T, Vesala T and Hari P 2004 A new feedback mechanism linking forests, aerosols, and climate *Atmos. Chem. Phys.* **4** 557–62
Liu X, Cheng Z, Yan L and Yin Z-Y 2009 Elevation dependency of recent and future minimum surface air temperature trends in the Tibetan Plateau and its surroundings *Glob. Planet. Change* **68** 164–74
Lukeš P, Stenberg P and Rautiainen M 2013 Relationship between forest density and albedo in the boreal zone *Ecol. Modell* **261-262** 74–9
Mahmood R *et al* 2014 Land cover changes and their biogeophysical effects on climate *Int. J. Climatol.* **34** 929–53
Maja M M 2015 Volatile organic compounds emitted from silver birch of different provenances across a latitudinal gradient in Finland *Tree Physiol.* **2100** 1–12
Makarieva A M and Gorshkov V G 2007 Biotic pump of atmospheric moisture as driver of the hydrological cycle on land *Hydrol. Earth Syst. Sci. Discuss.* **11** 1013–33
Makarieva A M, Gorshkov V G, Sheil D, Nobre A D and Li B L 2013 Where do winds come from? A new theory on how water vapor condensation influences atmospheric pressure and dynamics *Atmos. Chem. Phys.* **13** 1039–56
Manara V, Beltrano M C, Brunetti M, Maugeri M, Sanchez-Lorenzo A, Simolo C and Sorrenti S 2015 sunshine duration variability and trends in Italy from homogenized instrumental time series (1936–2013) *J. Geophys. Res. Atmos.* **120** 3622–41
Marcolla B, Cescatti A, Manca G, Zorer R, Cavagna M, Fiora A, Gianelle D, Rodeghiero M, Sottocornola M and Zampedri R 2011 Climatic controls and ecosystem responses drive the inter-annual variability of the net ecosystem exchange of an alpine meadow *Agric. For. Meteorol.* **151** 1233–43
Marty C and Meister R 2012 Long-term snow and weather observations at Weissfluhjoch and its relation to other high-altitude observatories in the Alps *Theor. Appl. Climatol.* **110** 573–83
Morris C E, Conen F, Alex Huffman J, Phillips V, Pöschl U and Sands D C 2014 Bioprecipitation: a feedback cycle linking Earth history, ecosystem dynamics and land use through biological ice nucleators in the atmosphere *Glob. Chang. Biol.* **20** 341–51
Oyler J W, Dobrowski S Z, Ballantyne A P, Klene A E and Running S W 2015 Artificial amplification of warming trends across the mountains of the western United States *Geophys. Res. Lett.* **42** 153–61
Peng S-S, Piao S, Zeng Z, Ciais P, Zhou L, Li L Z X, Myneni R B, Yin Y and Zeng H 2014 Afforestation in China cools local land surface temperature *Proc. Natl Acad. Sci. USA* **111** 2915–9
Pepin N *et al* 2015 Elevation-dependent warming in mountain regions of the world *Nat. Clim. Chang.* **5** 424–30
Pepin N and Losleben M 2002 Climate change in the Colorado Rocky Mountains: free air versus surface temperature trends *Int. J. Climatol.* **22** 311–29
Philipona R 2013 Greenhouse warming and solar brightening in and around the Alps *Int. J. Climatol.* **33** 1530–7
Philipona R, Behrens K and Ruckstuhl C 2009 How declining aerosols and rising greenhouse gases forced rapid warming in Europe since the 1980s *Geophys. Res. Lett.* **36** L02806
Pielke R A 2005 Atmospheric science. Land use and climate change *Science* **310** 1625–6
Qin J, Yang K, Liang S and Guo X 2009 The altitudinal dependence of recent rapid warming over the Tibetan Plateau *Clim. Change* **97** 321–7
Rangwala I and Miller J R 2012 Climate change in mountains: a review of elevation-dependent warming and its possible causes *Clim. Change* **114** 527–47
Rangwala I, Sinsky E and Miller J R 2013 Amplified warming projections for high altitude regions of the northern hemisphere mid-latitudes from CMIP5 models *Environ. Res. Lett.* **8** 024040
Rangwala I, Sinsky E and Miller J R 2015 Variability in projected elevation dependent warming in boreal midlatitude winter in CMIP5 climate models and its potential drivers *Clim. Dyn.* **46** 2115–22
Ruckstuhl C, Philipona R, Behrens K, Collaud Coen M, Dürr B, Heimo A, Mätzler C, Nyeki S, Ohmura A, Vuilleumier L, Weller M, Wehrli C and Zelenka A 2008 Aerosol and cloud effects on solar brightening and the recent rapid warming *Geophys. Res. Lett.* **35** L12708
Sakowska K, Vescovo L, Marcolla B, Juszczak R, Olejnik J and Gianelle D 2014 Monitoring of carbon dioxide fluxes in a subalpine grassland ecosystem of the Italian Alps using a multispectral sensor *Biogeosciences* **11** 4695–712
Schwaab J, Bavay M, Davin E, Hagedorn F, Hüsler F, Lehning M, Schneebeli M, Thürig E and Bebi P 2014 Carbon storage versus albedo change: radiative forcing of forest expansion in temperate mountainous regions of Switzerland *Biogeosciences* **11** 10123–65
Sitzia T 2009 *Ecologia e gestione dei boschi di neoformazione nel paesaggio del Trentino* (Trento: Provincia Autonoma di Trento - Servizio Foreste e Fauna)
Spracklen D V, Bonn B and Carslaw K S 2008 Boreal forests, aerosols and the impacts on clouds and climate *Philos. Trans. A. Math. Phys. Eng. Sci.* **366** 4613–26
Tasser E, Walde J, Tappeiner U, Teutsch A and Noggler W 2007 Land-use changes and natural reforestation in the Eastern Central Alps *Agric. Ecosyst. Environ.* **118** 115–29
Unger N 2014 Human land-use-driven reduction of forest volatiles cools global climate *Nat. Clim. Chang.* **4** 907–10
Verma S B 1989 Aerodynamic resistances to transfers of heat, mass and momentum *Estimation of Areal Evapotranspiration* ed T A Black (Wallingford: IAHS) pp 13–20
Wang Q, Fan X and Wang M 2013 Recent warming amplification over high elevation regions across the globe *Clim. Dyn.* **43** 87–101
Wang Q, Fan X and Wang M 2016 Evidence of high-elevation amplification versus Arctic amplification *Nat. Publ. Gr.* **6** 1–8

Wilson K B *et al* 2002 Energy partitioning between latent and sensible heat flux during the warm season at FLUXNET sites *Water Resour. Res.* **38** 1–11
de Wit H A, Bryn A, Hofgaard A, Karstensen J, Kvalevåg M M and Peters G P 2014 Climate warming feedback from mountain birch forest expansion: reduced albedo dominates carbon uptake *Glob. Chang. Biol.* **20** 2344–55
You Q, Kang S, Pepin N, Flügel W-A, Yan Y, Behrawan H and Huang J 2010 Relationship between temperature trend magnitude, elevation and mean temperature in the Tibetan Plateau from homogenized surface stations and reanalysis data *Glob. Planet. Change* **71** 124–33
Yunusa I A M, Eamus D, Taylor D, Whitley R, Gwenzi W, Palmer A R and Li Z 2015 Partitioning of turbulent flux reveals contrasting cooling potential for woody vegetation and grassland during heat waves *Q. J. R. Meteorol. Soc.* **141** 2528–37
Zeng Z, Chen A, Ciais P, Li Y, Li L Z X, Vautard R, Zhou L, Yang H, Huang M and Piao S 2015 Regional air pollution brightening reverses the greenhouse gases induced warming-elevation relationship *Geophys. Res. Lett.* **42** 4563–72